2021 43rd Annual International Conference of the
IEEE Engineering in Medicine & Biology Society (EMBC)
Oct 31 - Nov 4, 2021. Virtual Conference

# Development of muscle connection components for implantable power generation system*

Genta Sahara, Akihiro Yamada, *Member, IEEE*, Yusuke Inoue, *Member, IEEE*, Yasuyuki Shiraishi, *Member, IEEE*, Wataru Hijikata, Aoi Fukaya, and Tomoyuki Yambe, *Member, IEEE*

***Abstract*—We have been developing an implantable power generation system that uses muscle contraction following electrical stimulation as a permanent power source for small implantable medical devices. However, if the muscle tissue is overloaded for power generation, the tissue may rupture or blood flow may be impaired. In this study, we developed a new muscle-connecting component that solves these problems. The new connection device has three rods attached to the muscle fibers, and the force exerted on the muscle fibers is converted from horizontal to vertical when the muscle contracts. We conducted simulations with a three-dimensional (3D) model, as well as pulse wave muscle measurements and in vivo tests using the actual muscle. The pulse wave in the connecting part and its downstream were optically measured from the muscle surface, and the blood flow was not obstructed. The 3D model simulations revealed that the distribution of stress was preferable compared with the case in which a rod was stuck vertically in the muscle. In the in vivo muscle tests, the metal rod and resin parts were attached to the muscle, and a load of up to approximately 9 N was applied to the connecting part. Consequently, the connecting part was stable and integrated with the muscle, and there was no damage in the muscle. Although no long-term or histological evaluations were conducted, the device may be useful because of the intramuscular power generation owing to the minimal load applied on the part connected with the muscle.**

## I. Introduction

Active implantable medical devices (AIMDs), such as cardiac pacemakers, are used to assist function and human disease treatments. Additional types of devices are expected to be developed, such as artificial organs (e.g., pancreas and retina) and monitoring devices. The power sources for these devices are internal batteries that need to be replaced surgically when they are depleted. Invariably, this imposes a physical and mental burden on the patient. Moreover, as batteries have limited power, their applications are limited.

Methods for a) generating power in the body and b) for the supply of power to AIMDs have been studied. In this regard, studies using heartbeats, respiratory movements, body temperature, blood glucose, and body movements, as energy sources [1–5] have been reported. However, each of these approaches involves problems such as invasiveness, low-energy density, and reduced durability.

In our research, we focused on the contraction of skeletal muscles induced by electrical stimulation [6]. A muscle is a tissue that converts body chemical energy into mechanical energy. Muscle contractions can generate more energy than electrical stimulation, and the orders for muscle contractions by electrical stimulation can be adjusted according to the power demands of the AIMDs. Therefore, internal power generation that is more active than that possible via the abovementioned methods is expected to be used in applications in vivo.

However, in previous studies that used muscle contraction and a piezoelectric power generator [7], the amount of generated power was small, and the required muscle mass was large. Given that the generator was combined between the tendon and the bone, the bone also moved when the muscle contracted. Therefore, only small contractions can be used. In addition, muscle contraction is better for generating large displacements at low speeds [8].

Therefore, in this study, we applied electromagnetic induction-type power generation to develop an in vivo power generation system using muscle fibers (Fig. 1). By extracting the displacement from the middle point of the muscle, large power is generated without moving the bone. Appropriate electrical stimulation of a section of muscle results in muscle contraction of that section only, and the surrounding relaxed muscle is passively extended, preventing involuntary movements of the bone.

In this system, it is necessary to attach the force extraction component directly to the muscle. When the muscle contracts and acts on the neighboring anatomical parts, a reaction force is exerted on the muscle itself. However, loading soft tissues, such as muscles, causes problems. Muscle tissue consists of muscle fibers in the direction of contraction, and is particularly vulnerable to the force of tearing between fibers [9]. Given that the distribution of blood vessels is also along the direction of the muscle fibers [10], attaching parts can impair the blood flow to the muscle fibers located upstream or downstream of the blood flow. However, there are no reports of permanent

*Research supported by the Cooperative Research Project Program of the Joint Usage/Research Center at the Institute of Development, Aging and Cancer, at the Tohoku University.

G. Sahara is with the Graduate School of Biomedical Engineering, Tohoku University, Sendai, Japan (phone: 81-22-717-8517; fax: 81-22-717-8518; e-mail: genta.sahara.q3@dc.tohoku.ac.jp).

A. Yamada, Y. Shiraishi, and T. Yambe are with the Institute of Development, Aging and Cancer, Tohoku University, Sendai, Japan (akihiro.yamada.e1@tohoku.ac.jp, yasuyuki.shiraishi.d1@tohoku.ac.jp, tomoyuki.yambe.a4@tohoku.ac.jp).

Y. Inoue is with the Advanced Medical Engineering Research Center, Asahikawa Medical University, Asahikawa, Japan (inoue@asahikawa-med.ac.jp).

W. Hijikata is with the School of Engineering, Tokyo Institute of Technology, Tokyo, Japan (hijikata.w.aa@m.titech.ac.jp).

A. Fukaya is with the Department of Clinical Engineering, Faculty of Engineering, Tohoku Bunka Gakuen University, Sendai, Japan (aoi@ce.tbgu.ac.jp).

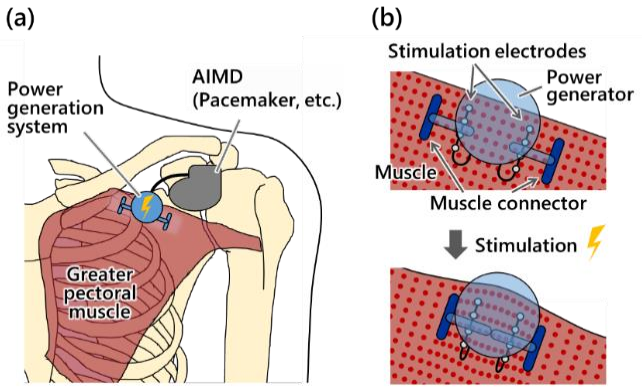


Figure 1. Example of implantable active power generation system.
(a) The system is implanted subcutaneously in the anterior chest at the same time as the AIMD and connected to the greater pectoral muscle. (b) The system **is** connected to a large muscle at two places away from the bones. Only the muscle between the connected parts is contracted by stimulation to drive the power generation mechanism.

and strong connections between muscle and artificial materials. Therefore, in this study, we propose the design and verify the effects of a component that does not concentrate stress in the muscle fiber direction and does not impede blood flow.

The new connection component, the muscle connector, has three rods that are perpendicular to the muscle fibers; one rod lifts the muscle, and two rods are placed next to it (Fig. 2). When the muscle contracts, the muscle tissue around the rod exerts a force on the rod in the direction perpendicular to the muscle fiber. It is necessary to penetrate the muscle in two places to let the central rod reach under the muscle. However, the blood flow is maintained because it is laterally displaced from the position directly upstream and downstream of the muscle contraction.

To evaluate the new connection parts, we performed blood flow evaluations by pulse wave muscle measurements, stress distribution simulations with 3D models, and load muscle contraction tests.

## II. Materials and Methods

### A. *Blood flow evaluation by pulse wave measurements in muscle*

In these studies, we complied with the institutional guidelines for the care and use of laboratory animals. Goat experiments were performed at Tohoku University and the study was approved by the Ethics Committee (2017AcA-052).

The goat (*Capra aegagrus hircus*) was a 76 kg male of the Japanese Saanen species. The target muscle was the latissimus dorsi muscle located on the cranial side of the trunk.

The goat was placed in a lateral position on an operating table. The goat was sedated by an intramuscular injection of 0.025 mg/kg of medetomidine, and anesthetized by inhalation of 2% isoflurane.

To emulate the situation in which muscle connectors were attached to the muscles, 3D-printed polylactic acid (PLA) resin parts, three 3.9 mm diameter screws, and two 5.3 mm diameter metal tubes were combined and attached to the latissimus dorsi muscle of the goat (Fig. 3).

A region of 2 cm on the surface of the muscle was picked up with tweezers, and the central screw was penetrated perpendicularly to the muscle fiber. The screw passed from the surface of the muscle to its inner parts and was then exposed again on its exit path.

The two screws on both sides that had a diameter of 5.3 mm owing to the metal tube made contact with the muscle surface to avoid pinching the muscle strongly. These were performed at two points in the latissimus dorsi muscle with a 5 cm interval along the direction of the muscle fibers.

A self-made reflective photoelectric pulse wave sensor (photoplethysmography) with a wavelength of 530 nm was used to investigate the blood flow in the muscle. Pulse waves were measured on the surface of the muscle and were pushed up by the central screw of the proximal and distal muscle connections and on the surface of the muscle between the two muscle connections.

### B. *Stress distribution simulation based on a 3D model*

The muscle is a hyperelastic body that is distorted nonlinearly with respect to stress. To simplify the conducted analysis, we assumed that the muscle was distorted linearly in the range in which the muscle-connecting parts were used.

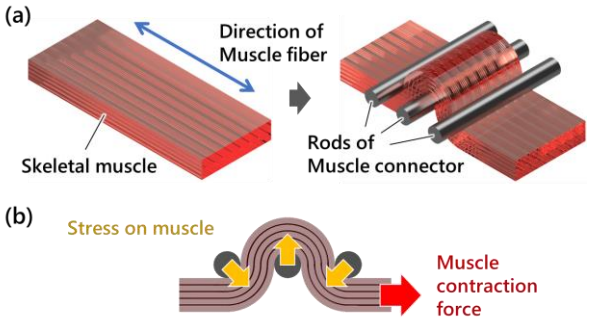


Figure 2. Concept of muscle connector.
(a) Selection of a part of the muscle with three rods perpendicular to the muscle fiber direction. (b) Direction of stress applied to the muscle changes during muscle contraction.

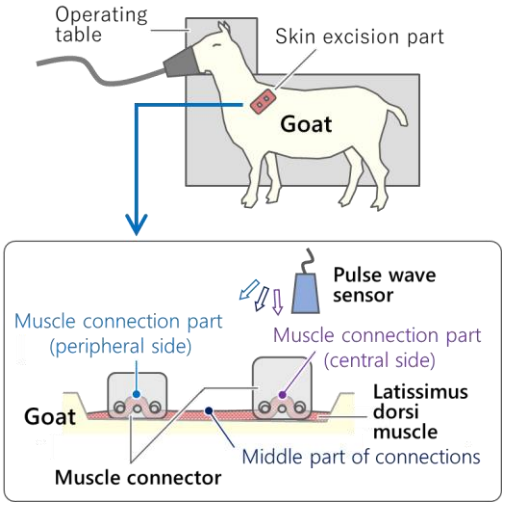


Figure 3. Muscle blood flow evaluation method. The latissimus dorsi muscle of the goat was exposed, and the blood flow of the muscle surface layer at and between the muscle connector installation sites was measured by photoelectric pulse waves.

To determine the approximate elastic modulus of the muscle, we investigated the relationship between stress and strain using the latissimus dorsi muscle in the goat, as mentioned above.

The excised muscle had an unloaded length of 49 mm and a cross-sectional area of 506 $mm^2$. One end of the muscle was fixed, the other end was connected to a load cell (LTS-2KA; Kyowa Electronic Instruments Co., Ltd., Tokyo, Japan), and the muscle was pulled and stretched through a strain gauge. The displacement of the strain gauge was measured with a laser displacement meter (LK-085; KEYENCE CO., Ltd., Osaka, Japan) and was regarded as the amount of muscle extension.

The average stress in each length was calculated from the cross-sectional area, and the strain–stress curve was derived. The curve was linearly approximated by the least squares method, and the elastic modulus was obtained from the slope.

Three-dimensional computer-aided design/computer-aided engineering software (Fusion360, Autodesk, California, USA) was used to create 3D models of the connecting parts and muscles and to analyze the stress applied to the muscles by the muscle connecting parts. The static stress analysis function of the finite element method was used.

The muscle model had a width of 20 mm, a thickness of 7 mm, a cross-sectional area of 140 $mm^2$, and the elastic modulus as identified above. It was fixed with connecting parts, and one end was pulled with a force of 2.5 N. The other end was free, and there was no interference between the bottom plate and the muscle. The center rod of the proposed muscle connector model was in contact with the posterior part of the muscle and had a diameter of 4 mm and a length of 20 mm. In the comparative model, three rods with a diameter of 4 mm were pierced perpendicularly to the muscle, and a total length of 20 mm was in contact with the muscle. This design was compared with our concept, as the simplest muscle connection method on the surface of the muscle. The contact condition between each rod and muscle was "separation," and the coefficient of friction was 0.5. The average element size was 3% of the constructed model size.

### C. Load test by muscle contraction

Based on the results of the simulation, the muscle connectors were manufactured with a 3D printer. The central screw was the same as that described above, and the screw fixing and the rods on both sides were made of PLA resin. The connecting parts were attached to the latissimus dorsi muscle of another goat (79 kg, male) at two locations in the muscle fiber direction at 5 cm intervals in the same manner as in the previous section. The anesthesia method was the same as in the previous section.

Given that an applied load assumes the initiation of the power generation mechanism of the system, a mechanism combining a slide mechanism, gears, and an electromagnetic induction generator was connected to the muscle connecting parts. To drive the mechanism, it is necessary to pull with a force of approximately 5–9 N. A stimulating needle electrode was inserted in the muscle between the connecting parts, and electrical stimulation was applied to cause the muscle to contract 28 times. The electrical stimulus was a continuous rectangular wave voltage with an amplitude of 2 V, a frequency of 50 Hz, pulse width of 0.2 ms, and a duration of 1 to 2 s. The muscles between the connecting parts were sufficiently contracted.

## III. Results

### A. Blood flow evaluation by pulse wave muscle measurements

Fig. 4 shows the pulse waves examined at the two muscle connections and the muscle surface between them. A stable pulse wave signal synchronized with the heartbeat was detected at all measurement sites. The amplitude of the pulse wave signal at the midpoint was larger than that of the muscle connection at the two locations.

Although the muscle was in a relaxed state at the time of blood flow measurements, the elasticity of the tissue caused some tension in the muscle.

### B. Stress distribution simulation based on a 3D model

The maximum tension applied to the muscle within the measurement range was 19 N, and the maximum muscle extension was 31.2 mm.

Fig. 5 shows the strain–stress curve and the approximate straight line obtained from the experiment of the goat latissimus dorsi muscle. Consequently, the elastic modulus (stress/strain) of the relaxed skeletal muscle was set to 0.047 MPa for use in the simulation.

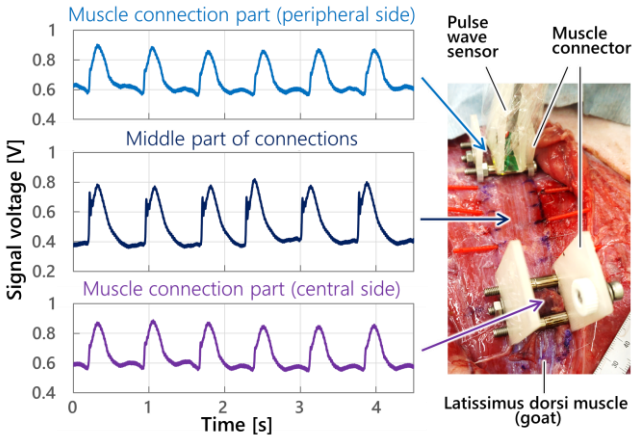


Figure 4. Pulse wave waveform and overview of pulse wave measurement. The pulse wave was measured with a photoelectric pulse wave sensor at the two muscle connection parts and the middle part.

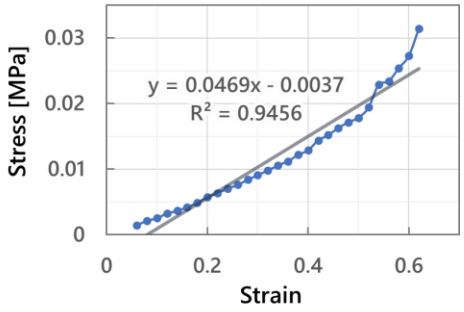


Figure 5. Derivation of elastic modulus of muscle.
Strain–stress curve was generated in an experiment using goat muscle. The approximate elastic modulus was obtained from the regression line.

Fig. 6(a) and (b) show an overview of the model and the results of the muscle stress distribution simulation. The colors were classified according to the von Mises stress, and the area where the stress was relatively concentrated was visualized. In the proposed muscle connector model (Fig. 6(a)), the stress received by the muscle was large around the rod on the load side and in the center. In the comparative model in which the rod pierced the muscle (Fig. 6(b)), stress was concentrated around the rod, and a gap was created between the rod and the muscle owing to the extension of the muscle.

### C. *Load test by muscle contraction*

Fig. 7(a) and 7(b) show the muscle connectors and muscles before and after the load experiment. The muscle connecting part did not detach from the muscle and did not move from the location where it was installed. In Fig. 7(b), the muscles were separated from the surrounding muscles and contracted so the distance between the muscle connectors was small.

Fig. 7(c) shows the cross-section of the muscle where the central rod was installed. There were no significant macroscopic findings—such as bleeding or rupture—that would indicate muscle tissue injury owing to the muscle connectors.

## IV. Discussion And Conclusion

We proposed a new component that could be connected to a muscle, extract the power without damaging the muscle, and verified it from the viewpoint of blood flow and stress.

The existence of blood flow is indispensable for living tissues, and the muscle-connecting parts were required to avoid interference with it. The signal of the photoelectric pulse wave sensor used for pulse wave measurements reflects the change in blood flow in the tissue up to a depth of several millimeters [11]. In the experiment, there was blood flow in the muscle tissue above the rods of the connecting parts, and the blood flow in the muscle between the connecting parts downstream and upstream was also confirmed.

The pulse wave signal of the muscle between the connecting parts was larger than that of the connecting parts. This blood flow decrease is presumed to be attributed to the damage inflicted to some blood vessel owing to the rod insertion and the influence of the pressure received from the rod. Even if the blood flow in the tissue is limited, if there is a certain amount of blood flow, the blood vessels will gradually strengthen and the blood flow will increase. In addition, during muscle contraction, the blood flow may be temporarily interrupted by the increase in the pressure received from the rod, but the tissue will not be damaged owing to the short-time interruption.

In the simulation, the feasibility of the concept of the muscle connector was confirmed from the viewpoint of the stress received by the muscle. Muscles are soft tissues with anisotropic tissue strength, and they easily break when subjected to stress in the direction of the muscle fibers [9]. From the stress concentration area of the comparative model, the local deformation of the muscle was large owing to the influence of tension. From these results, it is expected, that if a simple structure on which a force is exerted is placed in the muscle, the tensile stress concentrates in the direction of the muscle fiber, and the possibility that the muscle will tear along the fiber increases. Conversely, it was suggested that the

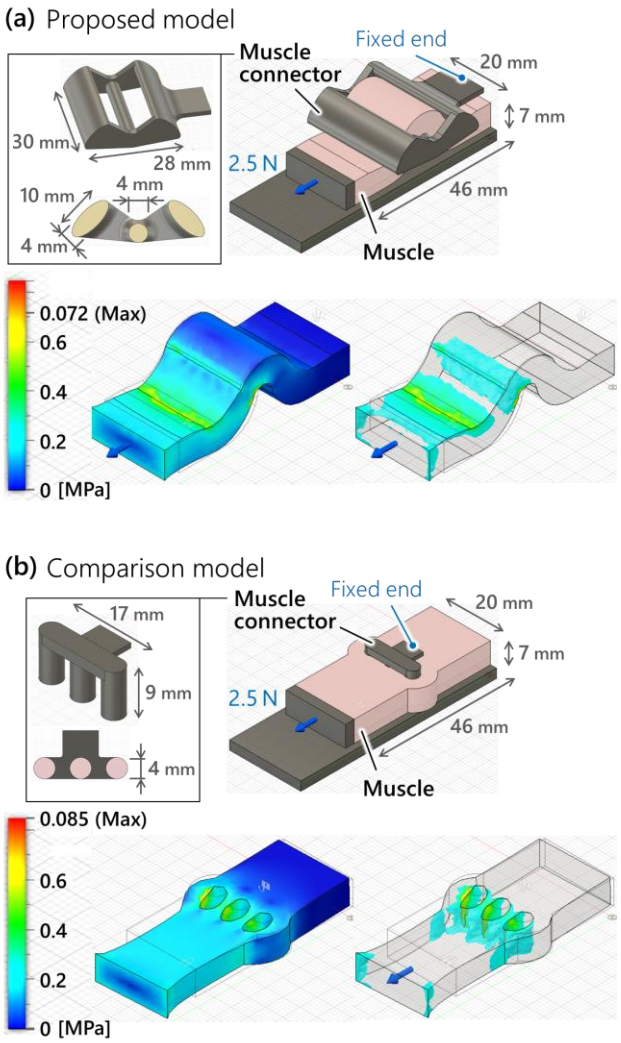


Figure 6. Simulation analysis of stress applied to the muscle by the muscle connector.
(a) Static stress analysis using a three-dimensional model of the proposed muscle connector. (b) Analysis of a simple muscle connector for comparison.

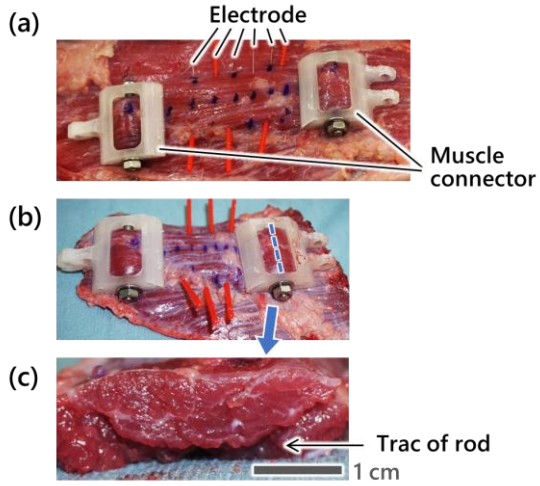


Figure 7. Muscle contraction load test of muscle connector.
(a) Overview before load test with muscle connector attached. (b) Overview after load test with muscles separated. Load of 5–9 N was applied 28 times. (c) Muscle cross-section of the central rod portion of the muscle connector after the load test.

proposed design of the connector with the rod in the horizontal direction exerts pressure and friction on the anterior and posterior sides of the muscle. The idea of changing the direction of the force exerted on the muscle and distributing the stress was shown to be effective. Given that the surface of the muscle was covered with a sturdy fascia, it seemed to have a mechanical strength that could withstand friction. In addition, because this design is symmetrical anteriorly and posteriorly, it works in a similar manner even when a force is exerted in the opposite direction.

Nonlinear stress analysis that can reflect the mechanical properties of muscles could not be completed, probably owing to the improper adjustment of the parameters. Therefore, in this simulation, the mechanical characteristics of the muscle tissue were simplified as an elastic body that deforms linearly, so the accuracy was not high, but the tendency of the stress distribution was considered sufficient. Even in the human body, forces are sometimes applied to muscles from the vertical direction of muscle fibers. For example, when a person sits on a solid chair, the gluteus maximus muscles receive the force attributed to the body weight given that it is being sandwiched between the ischium and the chair.

In the load experiment with muscles, it was found that muscle connectors were installed without any problems and were stable against loads. However, this is a preliminary result, and further investigation is needed to determine whether it is stable in the long term. The load of the periodic muscle contraction, which drives the power generation system, should be applied for several months and should be evaluated histologically.

Owing to the long-term foreign body reaction to artificial materials, the surrounding living tissues often atrophy. For example, the skin around an implantable medical device that has been under the skin for a long period of time becomes atrophied, thus exposing the device. One of the treatment methods is myocutaneous flap surgery. The muscle tissue is often used as the tough tissue part that covers the artifact [12, 13]. It is thus expected that the muscle tissue has durability against the muscle connecting parts. We also envision subcutaneous implantation of our implantable power generation system. A design with a low exposure risk of the system, including the muscle connector, by reducing protrusions to the shallow layer with the skin is required.

In this study, we only verified the basic principle of the muscle connection components and did not perform a comparative verification of various parameters related to the shape of the parts, such as the diameter and positioning of the rods. In the future, we will optimize such parameters and will select a detailed design. With regard to the outside of the device, if the shape of the area in contact with the surrounding tissue is curved, similar to a sphere, the foreign body reaction may be reduced [14]. We plan to select materials and surface treatments for long-term implantation tests.

When an artificial object is connected to a muscle so that a load can be applied, the force can be freely extracted from any muscle, and new applications that are not limited to power generation systems can be expected. Applying a safe and stable artificial load to soft tissue is a challenging subject, but the findings of this study have represent a possible solution.

## ACKNOWLEDGMENT

The authors would like to acknowledge Dr. Masahiro Tachi, Professor of Department of Plastic and Reconstructive Surgery, Tohoku University Graduate School of Medicine, for his help. We also thank Editage (www.editage.com) for English language editing.

## REFERENCES

[1] R. Tashiro, N. Kabei, K. Katayama, E. Tsuboi, and K. Tsuchiya, "Development of an electrostatic generator for a cardiac pacemaker that harnesses the ventricular wall motion," *J. Artif. Organs*, vol. 5, pp. 239–245, Sept. 2002.

[2] A. Zurbuchen, A. Pfenniger, A. Stahel, C. T. Stoeck, S. Vandenberghe, V. M. Koch, and R. Vogel, "Energy Harvesting from the Beating Heart by a Mass Imbalance Oscillation Generator," *Ann. Biomed. Eng.*, vol. 41, pp. 131–141, July 2012.

[3] H. Zhang, X. S. Zhang, X. Cheng, Y. Liu, M. Han, X. Xue, S. Wang, F. Yang, A. S. Smitha, H. Zhang, and Z. Xu, "A flexible and implantable piezoelectric generator harvesting energy from the pulsation of ascending aorta," *Nano Energy*, vol. 12, pp. 296–304, Jan. 2015.

[4] E. Häsler, L. Stein, and G. Harbauer, "Implantable physiological power supply with PVDF film," *Ferroelectrics*, vol. 60, no. 1, pp. 277–282, 1984.

[5] A. Nasiri, S. A. Zabalawi, and D. C. Jeutter, "A linear permanent magnet generator for powering implanted electronic devices," *IEEE Trans. Power Electron.*, vol. 26, no. 1, pp. 192–199, Jan. 2011.

[6] G. Sahara, W. Hijikata, K. Tomioka, and T. Shinshi, "Implantable power generation system utilizing muscle contractions excited by electrical stimulation," Proceedings of the Institution of Mechanical Engineers, Part H: *J. Eng. Med.*, vol. 230, no. 6, pp. 569–578, May 2016.

[7] B. E. Lewandowski, K. L. Kilgore, and K. J. Gustafson, "In Vivo Demonstration of a Self-Sustaining, Implantable, Stimulated-Muscle-Powered Piezoelectric Generator Prototype," *Ann. Biomed. Eng.*, vol. 37, pp. 2390–2401, Aug. 2009.

[8] K. A. P. Edman, "Double-hyperbolic force-velocity relation in frog muscle fibres," *J. Physiol.*, vol. 404, no. 1, pp. 301–321, Oct. 1988.

[9] W. Liu, Z. Yang, P. Li, J. Zhang, and S. Jiang, "Mechanics of tissue rupture during needle insertion in transverse isotropic soft tissue," *Med. Biol. Eng. Comput.*, vol. 57, pp. 1353–1366, Feb. 2019.

[10] T. C. Skalak and G. W. Schmid-Schönbein, "The microvasculature in skeletal muscle. IV. A model of the capillary network," *Microvascular Res.*, vol. 32, no. 3, pp. 333–347, Nov. 1986.

[11] M. Sandberg, Q. Zhang, J. Styf, B. Gerdle, and L.-G. Lindberg, "Non-invasive monitoring of muscle blood perfusion by photoplethysmography: evaluation of a new application," *Acta Physiol. Scandinavica*, vol. 183, no. 4, pp. 335–343, Mar. 2005.

[12] A. Viol, S. P. Pradka, S. P. Baumeister, D. Wang, K. E. Mo-yer, R. D. Zura, S. A. Olson, M. R. Zenn, S. L. Levin, and D. Erdmann, "Soft-Tissue Defects and Exposed Hardware: A Review of Indications for Soft-Tissue Reconstruction and Hardware Preservation," *Plastic Reconstruct. Surgery*, vol. 123, no. 4, pp. 1256–1263, Apr. 2009.

[13] T. Yamamoto, T. Saito, R. Ishiura, and T. Iida, "Quadruple-component superficial circumflex iliac artery perforator (SCIP) flap: A chimeric SCIP flap for complex ankle reconstruction of an exposed artificial joint after total ankle arthroplasty," *J. Plastic Reconstruct. Aesthetic Surgery*, vol. 69, no. 9, pp. 1260–1265, Sept. 2016.

[14] O. Veiseh, J. C. Doloff, and D. G. Anderson, "Size- and shape-dependent foreign body immune response to materials implanted in rodents and non-human primates," *Nature Materials*, vol. 14, pp. 643–651, May 2015.